# *In vivo* Margin Assessment during Partial Mastectomy Breast Surgery Using Raman Spectroscopy

Abigail S. Haka,[1] Zoya Volynskaya,[1] Joseph A. Gardecki,[1] Jon Nazemi,[1] Joanne Lyons,[2] David Hicks,[2] Maryann Fitzmaurice,[3] Ramachandra R. Dasari,[1] Joseph P. Crowe,[2] and Michael S. Feld[1]

[1]George R. Harrison Spectroscopy Laboratory, Massachusetts Institute of Technology, Cambridge, Massachusetts and [2]Cleveland Clinic Foundation, [3]University Hospitals of Cleveland and Case Western Reserve University, Cleveland, Ohio

## Abstract

**We present the first demonstration of *in vivo* collection of Raman spectra of breast tissue. Raman spectroscopy, which analyzes molecular vibrations, is a promising new technique for the diagnosis of breast cancer. We have collected 31 Raman spectra from nine patients undergoing partial mastectomy procedures to show the feasibility of *in vivo* Raman spectroscopy for intraoperative margin assessment. The data was fit with an established model, resulting in spectral-based tissue characterization in only 1 second. Application of our previously developed diagnostic algorithm resulted in perfect sensitivity and specificity for distinguishing cancerous from normal and benign tissues in our small data set. Significantly, we have detected a grossly invisible cancer that, upon pathologic review, required the patient to undergo a second surgical procedure. Had Raman spectroscopy been used in a real-time fashion to guide tissue excision during the procedure, the additional reexcision surgery might have been avoided. These preliminary findings suggest that Raman spectroscopy has the potential to lessen the need for reexcision surgeries resulting from positive margins and thereby reduce the recurrence rate of breast cancer following partial mastectomy surgeries.** (Cancer Res 2006; 66(6): 3317-22)

## Introduction

Breast cancer is the most common women's cancer in the United States, the second most common cause of cancer death in women (after lung cancer), and the main cause of death in women ages 45 to 55 years (1). Breast cancer surgery has changed dramatically over the past several decades and continues to evolve. With the emergence of breast-conserving surgical techniques, such as partial mastectomy, women may now preserve their breast without compromising survival. Partial mastectomy refers to surgical removal of the tumor and is typically followed by radiation therapy to eradicate any residual disease. Several modern, prospective, randomized clinical trials directly comparing partial mastectomy with traditional modified radical mastectomy, removal of the entire breast, have shown equivalent survival rates (2). The goal of partial mastectomy is to provide a low rate of cancer recurrence in the treated breast while maintaining good cosmesis.

In partial mastectomy procedures, complete surgical excision of the primary tumor is the major determinant of the rate of local cancer recurrence. Minimizing the amount of breast tissue removed is the main factor in preserving cosmetic appearance. Thus, in successful partial mastectomy surgery, complete resection of the cancer must be balanced with tissue conservation. To ensure that all malignant tissue is removed, a small margin of normal breast tissue surrounding the lesion is excised. To verify that the surgeon removed the entire malignant lesion, a pathologist performs an assessment of the tissue margins. Margin status is gauged by pathologic examination of the border of the excised lesion. This is a two-step process. The first step is intraoperative gross (macroscopic) examination; the second step is postoperative histologic (microscopic) examination of the margins. Achieving negative resection margins, typically defined as the absence of either invasive or intraductal cancer, provides lower associated rates of local recurrence following partial mastectomy (3–7). Positive or unknown histologic margins usually prompt reexcision surgery because such patients are at higher risk for local recurrence even when radiation therapy is administered. In clinical practice, as many as 20% to 55% of patients undergoing partial mastectomy require a second surgical procedure due to positive margins indicative of incomplete cancer resection that were missed on intraoperative margin assessment (8).

As a result, there are numerous approaches focused on enhancing intraoperative margin assessment. Gross inspection of the specimen in the operating room, with or without frozen section analysis, may permit identification of positive or close margins and immediate reexcision. However, routine frozen section analysis is time-consuming and can lead to inadequate assessment of tumor margins in large specimens and loss of diagnostic material in small specimens (9–11). Time-intensive techniques, such as frozen section analysis, also have the disadvantage of prolonging the surgical procedure and thereby the time the patient remains anesthetized. Therefore, intraoperative techniques that can provide real-time feedback are under investigation. Intraoperative ultrasound may assist in assuring negative margins, although it is generally of low resolution and, thus, its use does not preclude the presence of microscopic tumor seen on histologic examination (12). Sehgal et al. (13) used tissue echogenicity, the angular variance in echogenicity around the circumference of the lesion, and the patient's age to obtain a sensitivity and specificity of 95% and 63%, respectively. Optical techniques may assist in intraoperative margin assessment as they are also capable of providing immediate diagnosis and have the potential to provide high-resolution information. Currently, a variety of optical imaging and spectroscopic techniques are being explored to improve breast cancer diagnosis (14–24). However, few have been applied to surgical margin assessment. Optical techniques use visible or near-IR light and provide chemical information about the tissue being studied. Preliminary *in vivo* investigations have examined the efficacy of diffuse reflectance spectroscopy in the diagnosis of breast lesions,

**Requests for reprints:** Michael S. Feld, George R. Harrison Spectroscopy Laboratory, Massachusetts Institute of Technology, NW-14, 166 Albany Street, Cambridge, MA 02139. Phone: 617-253-7700; Fax: 617-253-4513; E-mail: mxf39@case.edu.



doi:10.1158/0008-5472.CAN-05-2815

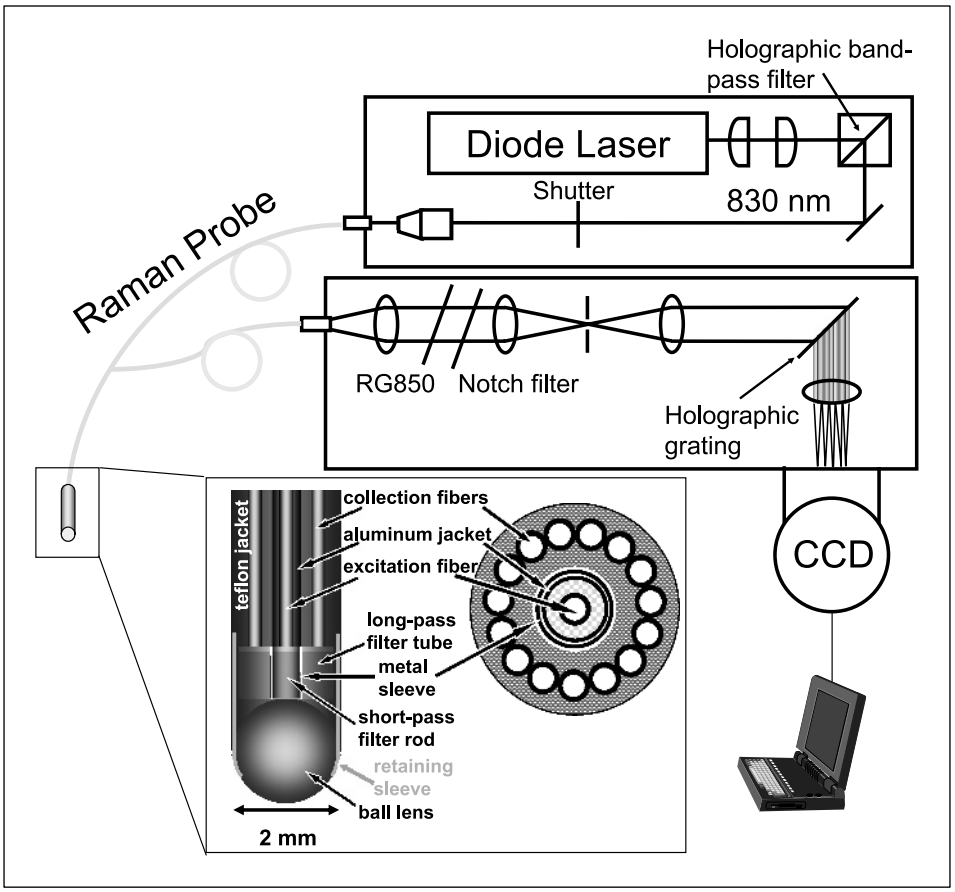


**Figure 1.** Schematic of the clinical Raman system and optical fiber Raman probe.

as well as in the assessment of tumor margins (23). Diffuse reflectance spectroscopy monitors changes in the absorption and reduced scattering coefficients among tissues with different pathologies. The study reports a sensitivity and specificity of 67% and 79%, respectively.

Raman spectroscopy is an optical modality capable of providing detailed quantitative chemical information about a tissue sample. It is particularly amenable to *in vivo* measurements, as the powers and excitation wavelengths used are nondestructive to the tissue and have a relatively large penetration depth (25). Several laboratories have investigated the use of Raman spectroscopy for the examination of a variety of breast pathologies (26–30).

Our previous research showed the ability of Raman spectroscopy to accurately diagnose normal, benign, and malignant lesions of the breast *ex vivo* in a laboratory setting with high sensitivities and specificities (31). Our approach relies on the use of a spectroscopic model of breast tissue (32). This model fits macroscopic tissue spectra with a linear combination of basis spectra derived from Raman microscopy of various breast tissue components. Specifically, the model includes Raman spectra of the epithelial cell cytoplasm, the cell nucleus, fat, β-carotene, collagen, calcium hydroxyapatite, calcium oxalate dihydrate, cholesterol-like lipid deposits, and water. Modeling of the Raman spectrum yields fit coefficients that reflect the chemical makeup of the lesion, which is, in turn, associated with morphologic changes that pathologists routinely rely on to diagnose disease. Tissue composition extracted through modeling was used as the basis of a diagnostic algorithm capable of differentiating between normal, benign, and malignant breast tissues. The fit coefficients for the basis spectra of fat and collagen were found to be the key diagnostic variables in distinguishing pathologies. The resulting diagnostic algorithm, which classifies tissues *ex vivo* according to specific pathologic diagnoses, achieved a sensitivity of 94%, a specificity of 96%, and an overall accuracy of 86% (108 of 126).

The excellent results of this study supported moving the technique to a clinical setting for further testing of its efficacy in breast cancer detection. This was made possible by the recent development of Raman optical fiber probes that enable acquisition of clinical data in real-time with good signal-to-noise ratios (33). Although Raman spectroscopy has been recognized as a powerful biomedical tool for more than a decade, *in vivo* studies have generally been limited to skin or sites that are accessible with bulk optic geometries (34–38). The recent development of a small-diameter, high-throughput Raman probe, with excellent filtering capabilities to reject unwanted signals generated within the probe itself, provides the ability to study remote organs with real-time diagnostic capability (33).

In this article, we present the first demonstration of *in vivo* collection of Raman spectra of breast tissue. Data were collected during partial mastectomy surgeries to show the feasibility of *in vivo* Raman spectroscopy for intraoperative margin assessment. The research serves to extend and confirm the results of our *ex vivo* studies. Results indicate that Raman spectroscopy has the potential to aid in intraoperative tumor resection. Accurate *in vivo* margin assessment techniques will reduce the number of reexcision procedures necessary to achieve negative partial mastectomy

margins. They may also extend partial mastectomy to those women who do not harbor sufficiently small or localized breast cancers to qualify for partial mastectomy by current standards.

## Materials and Methods

This study uses partial mastectomy surgery to show the feasibility of *in vivo* Raman spectroscopy. A total of 30 Raman spectra were collected from nine patients, 29 from margins subsequently found to be negative on pathology examination and 1 spectrum from a margin subsequently found to be positive on pathology examination. Of the 29 negative margins, 21 were composed of normal breast tissue whereas 8 contained fibrocystic change. The one positive margin was diagnosed as high-grade ductal carcinoma *in situ* (DCIS). We are able to accurately fit all 30 spectra with our previously developed spectral model of breast (32).

Two spectra were excluded from the present analysis. The first, a benign papilloma, is a pathology not encountered in our previous studies and thus our diagnostic algorithm does not encompass this type of tissue. The benign papilloma predominately exhibited spectral features indicative of fat, such as a 1,747 $cm^{-1}$ C=O ester stretch, 1,654 $cm^{-1}$ C=C stretch, and 1,301 $cm^{-1}$ - $CH_2$-$CH_3$ bend/twist. The second was a margin noted by the pathologist to harbor significant cautery effects resulting from the surgical procedure. This was the only specimen where cautery of this degree was seen.

**Instrumentation.** The experimental system and optical fiber Raman probe, used for these procedures and shown in Fig. 1, are described in detail elsewhere (33). Briefly, light from an 830 nm diode laser (Process Instruments, Salt Lake City, UT) is collimated and then bandpass filtered (Kaiser Optical Systems, Inc., Ann Arbor, MI) before being focused into the excitation fiber of the Raman probe. The 4-m-long probe is <2 mm in diameter and consists of a single central excitation fiber surrounded by 15 collection fibers. All fibers are low-OH fused silica and have a 200 μm core diameter. The distal end of the probe is registered with a dual-filter module that rejects the intense interfering signals generated in the fibers. The probe is terminated with a sapphire ball lens, which collimates the excitation light and efficiently gathers and couples the Raman scattered light from the tissue into the collection fibers. The linear array of collection fibers at the proximal end is coupled to an f/1.8 spectrograph (Kaiser Optical Systems, f/1.8i) for dispersion onto a liquid nitrogen cooled, back-illuminated, deep-depletion charge-coupled device detector (Spec-10: 400BR, Roper Scientific, Trenton, NJ). Four Raman optical fiber probes were used in this study to permit data acquisition in multiple procedures on a single day.

**Clinical procedure.** Before each procedure, the experimental system was aligned and the probe was submitted for cold-gas ethylene oxide sterilization. Just before surgery, the proximal ends of the sterilized Raman probe were coupled to the experimental system. The distal end of the probe was kept sterile and placed in gentle contact with the margin tissue while spectra were acquired. All room and surgical lights were turned off during the measurements. The spectrally examined margin tissue was then excised by the surgeon and underwent conventional pathologic examination. The standard surgical practice of the surgeon in this study is to excise six additional sampling margins from the surgical cavity following removal of the main tumor specimen. Raman spectra were collected from several of these margins before excision and, thus, only tissue that would normally be excised during the procedure was removed. Each spectrum was collected for a total of 1 second. The data was analyzed in real time as detailed below and a spectral-based diagnosis was displayed within 1 second (39). A range of powers, 82 to 125 mW, was used depending on the throughput of the probe used. Following data acquisition, a volume of tissue corresponding roughly to that probed by the spectroscopic measurement was excised by the surgeon. The margin specimens were then fixed in formalin, routinely processed, and the histologic slides were examined by an experienced breast pathologist who was blinded to the outcome of the Raman spectroscopy analysis.

The clinical protocol was approved by both the Massachusetts Institute of Technology Committee on the Use of Humans as Experimental Subjects and the Institutional Review Board of the Cleveland Clinic Foundation, in accordance with an assurance filed with and approved by the Department of Health and Human Services. Informed consent was obtained from all subjects before the surgical procedures.

**Data processing.** Following each procedure, calibration data were collected for spectral corrections. Wave number calibration was established with a spectrum of 4-acetamidophenol. Chromatic intensity variations were corrected by collecting the spectrum of a tungsten white light source diffusely scattered by a reflectance standard ($BaSO_4$). The remaining probe

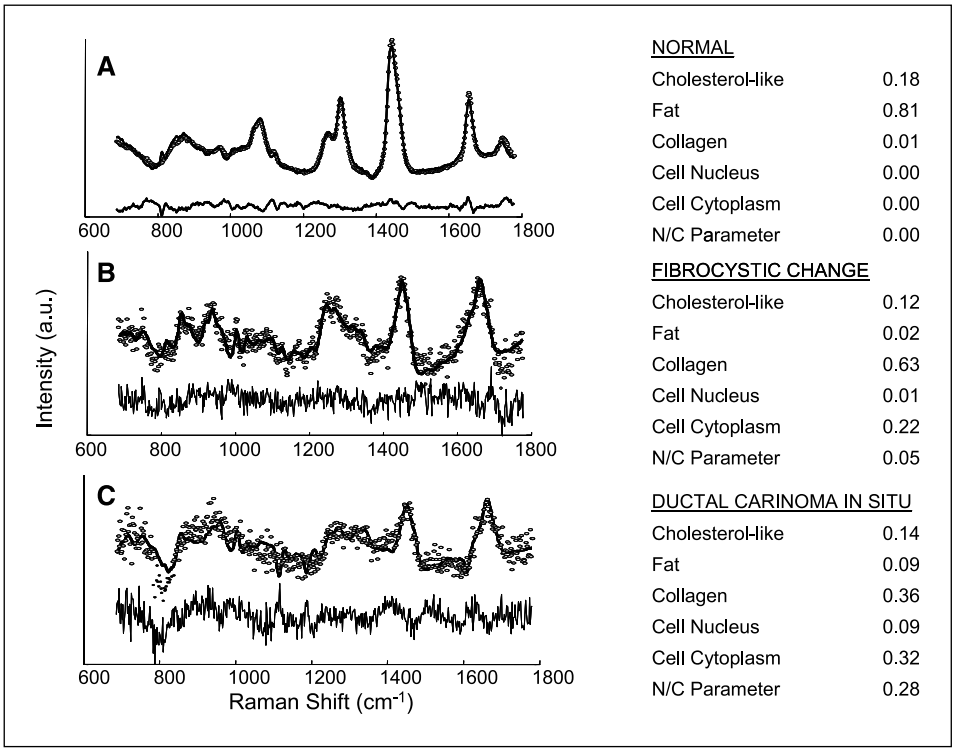


**Figure 2.** Normalized Raman spectra (*solid line*), model fit (*dotted line*), residual (shown below), and fit coefficients representative of (*A*) normal breast tissue, (*B*) fibrocystic change, and (*C*) DCIS.

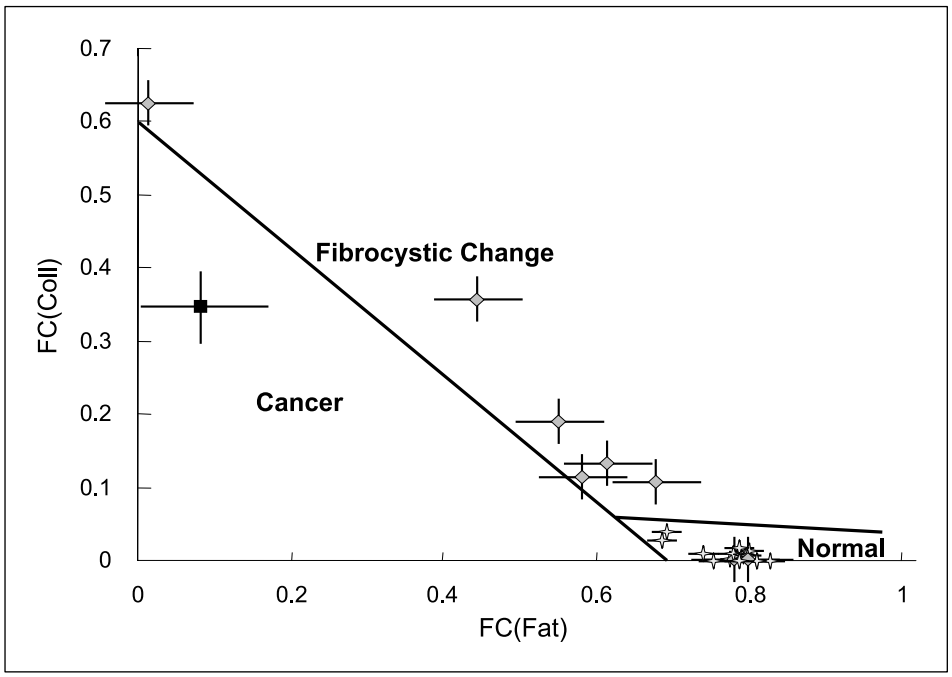


**Figure 3.** Scatter plot displaying the fat and collagen content for the *in vivo* Raman spectra acquired in this study. *Points,* normal (*stars*), fibrocystic change (*diamonds*), and DCIS (*square*); *bars,* SD.

background generated in the optical fibers was characterized by collecting the scattered excitation light from a roughened aluminum surface. This background was optimally subtracted from the data in an iterative loop by using a scaling factor related to the optical properties of the tissue (33). The tissue fluorescence background was modeled with a sixth-order polynomial. Finally, the data was fit via nonnegativity constrained least-squares minimization with the spectral model developed previously for the diagnosis of breast cancer (32). To accurately model the *in vivo* data, spectra of probe components, epoxy and sapphire, were included in the model. In accordance with our initial diagnostic study, the fit coefficients of fat, collagen, cell nucleus, epithelial cell cytoplasm, and cholesterol-like lipid deposits were normalized to sum to a total contribution of one. In the present study, the two types of microcalcifications, calcium hydroxyapatite and calcium oxalate dihydrate, were excluded from this normalization, as no microcalcification were present in the tissue samples used for the diagnostic algorithm development. We also observed larger contributions from β-carotene in our *in vivo* data than in our prior *ex vivo* data, and thus this component was excluded from normalization. Omission of β-carotene from the fit coefficient normalization was a modification to the real-time data analysis that was done intraoperatively.

To determine the error in our fit coefficients, we used a $\chi^2$ analysis (40). $\chi^2$ analysis is a well-known method for calculating the goodness of a fit as well as the error associated with model fitting. Error bars, 1 SD, are generated from this analysis. The Raman spectra in each diagnostic category have different signal-to-noise ratios; thus, mean errors are reported for each pathology. Fitting errors for the two diagnostic model components, fat and collagen, are 0.04 and 0.02 for normal specimen, 0.12 and 0.06 for fibrocystic change, and 0.18 and 0.10 for DCIS. Errors are slightly larger for fat than for collagen because the Raman spectrum of fat has more similarity to other model components than that of collagen.

## Results

Model fits to *in vivo* Raman spectra acquired from normal, benign, and malignant breast tissue are shown in Fig. 2. The difference between the measured spectrum and the model fit, the residual, is shown below each spectrum. The lack of significant structure in the residuals shows that the model accounts for the majority of the spectroscopic features observed and describes the data well. The fit coefficients, also displayed in Fig. 2, represent the amount that each model basis spectrum must be weighted to recreate the tissue spectrum, thereby providing insight into the chemical/morphologic makeup of the tissue.

Fit coefficients are a function of both the concentration of a particular model component and its Raman scattering cross-section (which indicates the strength of the signal at unit concentration). The fit coefficients of normal breast tissue exhibit a large contribution from fat. This is because normal breast tissue is predominately composed of adipocytes, cells containing large amounts of cytoplasmic fat, and also because relative to most other model components, fat has a large Raman scattering cross section. This explains the excellent signal-to-noise ratio evident in the spectrum acquired from normal breast tissue (Fig. 2A). There is more noise evident in spectra acquired from diseased tissue; however, they still yielded excellent model fits.

Fibrocystic change is a benign condition that can manifest itself as fibrosis (a scarring process characterized by an increased stromal component and thus by accumulation of collagen), adenosis (increase in the number of ductules), or cyst formation (dilation of ducts and lobules with fluid). The margin that harbors fibrocystic change shows an increase in the fit coefficients of collagen, due to fibrosis, and epithelial cell cytoplasm, as a consequence of adenosis. The fit coefficients of the positive margin, diagnosed as high-grade DCIS, also display an increase in the amount of epithelial cell cytoplasm. In our studies, the spectroscopic variable characterizing the nucleus-to-cytoplasm ratio, obtained by dividing the fit coefficient of the cell nucleus basis spectrum by the fit coefficient of the epithelial cell cytoplasm basis spectrum, is much larger for the cancerous specimen, shown in Fig. 2C, than for any of the fibrocystic lesions encountered in this study. A histologic signature of carcinoma is enlargement of cell nuclei, and thus a higher nucleus-to-cytoplasm ratio than seen in benign conditions. In fact, the nucleus-to-cytoplasm ratio is a criterion routinely used by pathologists in the diagnosis of breast cancer (41, 42).

**Table 1.** Comparison of pathologic diagnosis with that of the Raman diagnostic algorithm

| Raman diagnosis | Pathology | | |
|---|---|---|---|
| | Normal (21 spectra) | Fibrocystic change (8 spectra) | Cancer (1 spectrum) |
| Normal | 21 | 2 | 0 |
| Fibrocystic | 0 | 6 | 0 |
| Cancer | 0 | 0 | 1 |

NOTE: The Raman diagnostic algorithm results in an overall accuracy of 93% (28 of 30).

Figure 3 displays a scatter plot of the fit coefficients for collagen and fat, FC(Coll) and FC(Fat), respectively, for all data acquired in this study. Also shown are the decision lines that separate samples according to diagnoses. The diagnostic algorithm shown in Fig. 3 was developed previously using 126 spectra from 58 patients and is used in a prospective manner in this study (31). Table 1 compares the pathology diagnoses with those of the Raman diagnostic algorithm for our data set. The algorithm results in a sensitivity for detecting carcinoma of 100%, a specificity of 100%, and an overall accuracy of 93.3% (28 of 30). We note that although there is only one malignant sample in the present data set, this algorithm has been previously validated with 31 cancer specimens. The high-grade DCIS correctly identified by Raman spectroscopy was grossly invisible. Upon pathologic review, the finding that this margin was positive necessitated that the patient undergo a second surgery to excise the remaining cancer tissue. Had Raman spectroscopy been used in a real-time fashion to guide excision during the initial surgery, the additional procedure could have been avoided.

## Discussion

This pilot study is the first use of Raman spectroscopy to examine breast cancer *in vivo*. It clearly shows the feasibility of Raman spectroscopy as a clinical technique for real-time margin assessment during partial mastectomy surgery. The data exhibit good agreement with our previously developed spectral model and diagnostic algorithm. Studies with a larger patient pool are currently under way to further expand and validate our diagnostic algorithm in this and other clinical settings. And although complete postoperative pathologic examination of surgical margins will undoubtedly remain the standard of care for breast cancer surgery for the foreseeable future, we believe that the excellent results of this initial pilot study indicate that Raman spectroscopy has the potential to improve intraoperative margin assessment. This will likely occur first as an adjunct to and perhaps ultimately replacing intraoperative pathologic examination, thereby reducing the recurrence rate of breast cancer following partial mastectomy surgeries. As the first *in vivo* demonstration of Raman spectroscopy of breast tissue, this study has implications in addition to margin assessment. There are several areas where Raman spectroscopy may aid in breast cancer diagnosis and treatment. In particular, optical techniques are less invasive than current diagnostic procedures. The results of this study suggest the potential for transdermal needle measurements to afford breast cancer diagnosis. As opposed to standard biopsy, a spectroscopic transdermal needle measurement would have the advantage of providing immediate diagnosis. As a result, Raman spectroscopy has the potential to reduce both the likelihood of a nondiagnostic biopsy that would require repeat needle or surgical biopsy and patient anxiety by eliminating the currently unavoidable wait for a traditional histopathology diagnosis. Furthermore, with the development of minimally invasive breast cancer therapies, such as radiofrequency ablation, which relies on insertion of a thin metal probe into the breast, there is the potential that diagnosis and treatment could be done in a single procedure (43).

## Acknowledgments

Received 8/9/2005; revised 10/14/2005; accepted 1/9/2006.

**Grant support:** NIH grant HL-64675 and National Center for Research Resources program grant P41-RR-02594.

The costs of publication of this article were defrayed in part by the payment of page charges. This article must therefore be hereby marked *advertisement* in accordance with 18 U.S.C. Section 1734 solely to indicate this fact.

We thank Deborah Baynes, Jim Stanicky, and Richard Schule for assistance in the clinical procedures and the entire surgical staff at the Cleveland Clinic Foundation for their assistance in the research.

## References

1. Jemal A, Tiwari RC, Marray T, et al. Cancer statistics. CA Cancer J Clin 2004;54:8–29.
2. Early Breast Cancer Trialists' Collaborative Group. Effects of radiotherapy and surgery in early breast cancer. An overview of the randomized trials. N Engl J Med 1995;333:1444–55.
3. Gage I, Schnitt SJ, Nixon AJ, et al. Pathologic margin involvement and the risk of recurrence in patients treated with breast-conserving therapy. Cancer 1996;78:1921–8.
4. Park CC, Mitsumori M, Nixon A, et al. Outcome at 8 years after breast-conserving surgery and radiation therapy for invasive breast cancer: influence of margin status and systemic therapy on local recurrence. J Clin Oncol 2000;18:1668–75.
5. Smitt MC, Nowels KW, Zdeblick MJ, et al. The importance of the lumpectomy surgical margin status in long-term results of breast conservation. Cancer 1995; 76:259–67.
6. Anscher MS, Jones P, Prosnitz LR, et al. Local failure and margin status in early-stage breast carcinoma treated with conservation surgery and radiation therapy. Ann Surg 1993;218:22–8.
7. Borger J, Kemperman H, Hart A, et al. Risk factors in breast-conservation therapy. J Clin Oncol 1994;12: 653–60.
8. Walls J, Knox F, Baildam AD, et al. Can preoperative factors predict for residual malignancy after breast biopsy for invasive cancer? Ann R Coll Surg Engl 1995; 77:248–51.
9. Ferreiro JA, Gisvold JJ, Bostwick DG. Accuracy of frozen-section diagnosis of mammographically directed breast biopsies. Results of 1,490 consecutive cases. Am J Surg Pathol 1995;19:1267–71.
10. Johnson AT, Henry-Tillman R, Klimberg VS. Breast conserving surgery: optimizing local control in the breast with the assessment of margins. Breast Dis 2001; 12:35–41.
11. Klimberg VS, Westbrook KC, Korourian S. Use of touch preps for diagnosis and evaluation of surgical margins in breast cancer. Ann Surg Oncol 1998;5:220–6.
12. Klimberg VS, Harms S, Korourian S. Assessing margin status. Surg Oncol 1999;8:77–84.
13. Sehgal CM, Cary TW, Kangas SA, et al. Computer-based margin analysis of breast sonography for differentiating malignant and benign masses. J Ultrasound Med 2004;23:1201–9.
14. Fantini S, Walker SA, Franceschini MA, et al. Assessment of the size, position, and optical properties of breast tumors *in vivo* by non-invasive optical methods. Appl Opt 1998;37:1982–9.
15. Hebden JC, Veenstra H, Dehghani H, et al. Three-dimensional time-resolved optical tomography of a conical breast phantom. Appl Opt 2001;40:3278–87.
16. Quaresima V, Matcher SJ, Ferrari M. Identification and quantification of intrinsic optical contrast for near-infrared mammography. Photochem Photobiol 1998;67: 4–14.
17. Tromberg BJ, Coquoz O, Fishkin JB, et al. Non-invasive

measurements of breast tissue optical properties using frequency-domain photon migration. Philos Trans R Soc Lond B Biol Sci 1997;352:661–8.
**18.** Shah N, Cerussi A, Eker C, et al. Noninvasive functional optical spectroscopy of human breast tissue. Proc Natl Acad Sci U S A 2001;98:4420–5.
**19.** Ntziachristos V, Yodh AG, Schnall M, Chance B. Concurrent MRI and diffuse optical tomography of breast after indocyanine green enhancement. Proc Natl Acad Sci U S A 2000;97:2767–72.
**20.** Gupta PK, Majumder SK, Uppal A. Breast cancer diagnosis using $N_2$ laser excited autofluorescence spectroscopy. Lasers Surg Med 1997;21:417–22.
**21.** Majumder S, Gupta P, Jain B, Uppal A. UV excited autofluorescence spectroscopy of human breast tissues for discriminating cancerous tissue from benign tumor and normal tissue. Lasers Life Sci 1998;00:1–16.
**22.** Yang Y, Katz A, Celmer EJ, Zurawska-Szczepaniak M, Alfano RR. Fundamental differences of excitation spectrum between malignant and benign breast tissues. Photochem Photobiol 1997;66:518–22.
**23.** Bigio IJ, Bown SG, Briggs G, et al. Diagnosis of breast cancer using elastic-scattering spectroscopy: preliminary clinical results. J Biomed Opt 2000;5:221–8.
**24.** Yang Y, Katz A, Celmer EZ, Zurawska-Szczepaniak M, Alfano RR. Excitation spectrum of malignant and benign breast tissues: a potential optical biopsy approach. Lasers Life Sci 1997;7:115–27.
**25.** Hanlon EB, Manoharan R, Koo TW, et al. Prospects for *in vivo* Raman spectroscopy. Phys Med Biol 2000;45: R1–59.
**26.** Manoharan R, Shafer K, Perelman L, et al. Raman spectroscopy and fluorescence photon migration for breast cancer diagnosis and imaging. Photochem Photobiol 1998;67:15–22.
**27.** Frank CJ, McCreery RL, Redd DC. Raman spectroscopy of normal and diseased human breast tissues. Anal Chem 1995;67:777–83.
**28.** Frank CJ, Redd DC, Gansler TS, McCreery RL. Characterization of human breast biopsy specimens with near-IR Raman spectroscopy. Anal Chem 1994;66: 319–26.
**29.** Redd D, Feng Z, Yue K, Gansler T. Raman spectroscopic characterization of human breast tissues: implications for breast cancer diagnosis. Appl Spectrosc 1993;47:787–91.
**30.** Alfano RR, Liu CH, Sha W, et al. Human breast tissues studied by IR Fourier transform Raman spectroscopy. Lasers Life Sci 1991;4:23–8.
**31.** Haka AS, Shafer-Peltier KE, Fitzmaurice M, et al. Diagnosing breast cancer using Raman spectroscopy. Proc Natl Acad Sci U S A 2005;102:12371–6.
**32.** Shafer-Peltier K, Haka AS, Fitzmaurice M, et al. Raman microspectroscopic model of human breast tissue: implications for breast cancer diagnosis *in vivo*. J Raman Spectrosc 2002;33:552–63.
**33.** Motz JT, Hunter M, Galindo LH, et al. Optical fiber probe for biomedical Raman spectroscopy. Appl Opt 2004;43:542–54.
**34.** Caspers PJ, Lucassen GW, Bruining HA, et al. *In vitro* and *in vivo* Raman spectroscopy of human skin. Biospectroscopy 1998;4:S31–9.
**35.** Shim MG, Song L-MWK, Marcon NE, et al. *In vivo* near-infrared Raman spectroscopy: demonstration of feasibility during clinical gastrointestinal endoscopy. Photochem Photobiol 2000;72:146–50.
**36.** Buschman HP, Marple ET, Wach ML, et al. *In vivo* determination of the molecular composition of artery wall by intravascular Raman spectroscopy. Anal Chem 2000;72:3771–5.
**37.** Utzinger U, Heintzelman L, Mahadevan-Jansen A, et al. Near-infrared Raman spectroscopy for *in vivo* detection of cervical precancers. Appl Spectrosc 2001;55: 955–9.
**38.** Bakker Schut TC, Wolthuis R, Caspers PJ, et al. Real-time tissue characterization of the basis of *in vivo* Raman spectra. J Raman Spectrosc 2002;33:580–5.
**39.** Motz J, Gandhi SJ, Scepanovic O, et al. Real-time Raman system for *in vivo* disease diagnosis. J Biomed Opt 2005;10:031113–7.
**40.** Kenney JF, Keeping ES. Mathematics of statistics, Pt. 2, 2nd ed. Princeton (New Jersey): Van Nostrand; 1951.
**41.** Elston CW, Ellis IO. Pathological prognostic factors in breast cancer. I. The value of histological grade in breast cancer: experience from a large study with long-term follow-up. Histopathology 1991;19:403–10.
**42.** Hoda SA, Rosen PP. Practical considerations in the pathologic diagnosis of needle core biopsies of breast. Am J Clin Pathol 2002;118:101–8.
**43.** Fornage BD, Sneige N, Ross MI, et al. Small (< or = 2-cm) breast cancer treated with US-guided radiofrequency ablation: feasibility study. Radiology 2004;231: 215–24.